RSC Advances

PAPER

Cite this: *RSC Adv.*, 2024, **14**, 37062

Synergistic effects of hierarchical micro/nanostructures and PDMS/lubricant composites for superior tribological and wetting performance on aluminum

Sung-Jun Lee, Dawit Zenebe Segu and Chang-Lae Kim *

Received 5th June 2024
Accepted 5th November 2024

DOI: 10.1039/d4ra04121f

rsc.li/rsc-advances

In this study, we propose a method to enhance the friction and wetting properties of aluminum surfaces with micro-/nanostructures by coating them with a PDMS/lubricant composite. Hierarchical micro/nanostructures were formed on the aluminum surface through an etching process, and coating solutions were prepared by mixing xylene and the PDMS/lubricant composites in various ratios. The surface morphology, roughness, and wettability of the coated specimens were analyzed, and their friction and wear characteristics were evaluated under dry and lubricated conditions. The results showed that the PDMS/lubricant composite coating significantly reduced friction and wear under both dry and lubricated conditions owing to the formation of a stable lubricating film. Additionally, the hierarchical micro/nanostructures formed by the etching process improved hydrophobicity and self-cleaning ability. The coated surface exhibited selective wettability towards water and oil, offering various advantages such as prevention of contamination, prevention of wear and performance degradation caused by lubricant oxidation, and enhanced corrosion resistance. The findings of this study are expected to contribute to the development of lightweight mechanical-component technologies with improved durability and wear resistance.

1. Introduction

The modern mechanical industry is constantly pursuing advancements, with performance enhancement and efficiency improvement considered pivotal elements.[1,2] Among these, lightweight mechanical components play a crucial role in reducing the energy consumption and enhancing the performance.[3–5] However, this lightweight process is accompanied by decreased durability.[6,7] In particular, in high-performance devices such as internal combustion engines, the piston acts as a critical component, and its lightweight significantly affects the overall system performance.[8] Aluminum, which is light yet strong, is widely used for this purpose. However, the inherent friction and wear properties of aluminum are substantially inferior to those of other metals, leading to various operational issues.[9,10] Lubrication has been used to resolve these issues.[11,12] This reduces the friction between the piston and cylinder walls, enabling stable operation. Lubrication also plays a vital role in heat dispersion and corrosion prevention, mitigating direct contact and impact on aluminum, thereby facilitating precise operation and minimizing vibrations and noise.[13,14]

Nevertheless, the high viscosity of lubricants used in internal combustion engines leads to reduced fuel efficiency and complexity of waste lubricant treatment processes.[15] Moreover, waste lubricants pose environmental pollution issues, necessitating solutions.[16] Recently, there has been a shift towards low-viscosity oils to improve the lubrication fuel efficiency in internal combustion engines.[17] Although the use of low-viscosity lubricants offers various advantages, such as reduced energy consumption, according to the Stribeck curve, it can lead to an increase in wear owing to an increase in the friction coefficient within a certain range.[18,19] The transition to aluminum for lightweight mechanical parts and the use of low-viscosity lubricants for energy consumption reduction interact in a complex manner, posing challenges in practical applications.

To address these challenges, various surface modification techniques, such as anodization, plasma electrolytic oxidation, laser surface texturing, and composite coating applications have been used to improve the friction characteristics and durability of aluminum surfaces.[20] While these methods have shown promise in improving the wear resistance, corrosion resistance, and friction behavior of aluminum, and they have limitations in terms of complex processes, high costs, or substrate geometry and scalability.

Department of Mechanical Engineering, Chosun University, Gwangju, 61452, Republic of Korea. E-mail: kimcl@chosun.ac.kr

Recent studies have explored the potential of achieving synergistic effects by combining surface texturing and low-surface-energy coatings to enhance the tribological performance of mechanical component materials. Wang *et al.* demonstrated that combining laser texturing with superhydrophobic coating significantly reduces the friction coefficient and wear loss of steel substrates.[21] The textured surface provided reservoirs that could form lubricating films under water lubrication, while the superhydrophobic coating improved the surface's wear resistance and hydrophobicity. Similarly, Boinovich *et al.* developed a method for fabricating superhydrophobic oxide surfaces on aluminum alloys to enhance their resistance to erosion corrosion.[22] They reported that the developed coating exhibited excellent superhydrophobicity and enhanced corrosion resistance.

Despite these promising results, the synergistic effects of combining hierarchical micro-/nanostructures formed by etching with PDMS/lubricant composite coatings for aluminum surface modification have not been extensively studied. This approach has the potential to offer several benefits. First, the etching process can generate three-dimensional hierarchical structures with micro-and nanoscale features, significantly increasing the surface area and roughness.[23–27] This can improve the adhesion between the PDMS/lubricant composite coating and aluminum substrate, enhancing durability and wear resistance. Second, the micro/nanostructures can contribute to improved hydrophobicity and oleophilicity by increasing the contact area with oil.[28] This selective wettability can be further enhanced by the low surface energy of the PDMS/lubricant composite, resulting in a surface with excellent water repellency and oil affinity. Third, the PDMS/lubricant composite coating can act as a reservoir for the lubricant, continuously supplying it to the contact interface during sliding.[29] The micro/nanostructures can help retain the lubricant, maintain a stable lubricating film, and reduce friction and wear. Additionally, incorporating a lubricant into the PDMS matrix can potentially address issues associated with low-viscosity lubricants by providing a localized lubricant supply at the contact interface, thereby reducing the dependence on lubricants.

In this study, we propose a novel approach to enhance the friction and wetting characteristics of aluminum surfaces by combining hierarchical micro/nanostructures formed *via* chemical etching with PDMS/lubricant composite coatings. In this experiment, PDMS and lubricant composite materials mixed in various ratios with xylene were coated onto etched aluminum to form a surface-coating layer. Xylene acted as an excellent solvent, providing necessary viscosity control and uniformity during the coating process.[30,31] The surface morphology, roughness, and wettability of coated specimens were analyzed, and friction and wear characteristics were evaluated under dry and lubricated conditions. We investigated the synergistic effects of hierarchical surface structures and PDMS/lubricant composite coatings on the tribological performance, self-cleaning properties, and selective wettability of aluminum surfaces. The results of this study are expected to contribute to the development of advanced surface modification strategies for lightweight aluminum components with enhanced durability, wear resistance, and multifunctional characteristics, particularly in the context of the challenges arising from the transition to low-viscosity lubricants and the increasing demand for energy-efficient and environmentally friendly solutions.

2. Materials and methods

2.1 Materials

Al 5052 (35 mm × 35 mm × 1 mm) was used as the base substrate, sodium hydroxide (Beads, 98%), hydrochloric acid (3 mol L^{-1}), and xylene (99.5%) were purchased from SAMCHUN Chemicals, Republic of Korea. The PDMS base and curing agent (Sylgard 184) were purchased from DOW Hitech, Republic of Korea. The lubricant (Super Lube) was purchased from SYNCO, USA. Lubricant (KF-96, 100 CS) was purchased from ShinEtsu, Republic of Korea.

2.2 Specimen fabrication

In this study, we aimed to enhance wear resistance by integrating a coating of a PDMS/lubricant composite and low-viscosity lubrication onto an aluminum (Al) substrate with micro/nano surface structures. The methodology was implemented as follows: Fig. 1 shows an overview of the specimen fabrication process. The Al substrates were ultrasonically cleaned with ethanol and dried in a hot air oven. The cleaned substrate was immersed in 1 M NaOH solution for approximately one minute, followed by a 6 minutes immersion in a 3 M HCl solution for etching. The etched Al specimens were then immersed in 1 M NaOH solution for one minute. Subsequently, the Al specimens were immersed in hot water (>90 °C) for six minutes. After completing this process, the Al specimens were dried in an oven at 70 °C for 30 min. The PDMS composite material was prepared by mixing the base and curing agent at a 10 : 1 ratio to prepare the PDMS solution. The lubricant was then mixed with the blended PDMS in a 10 : 1 weight ratio to manufacture the PDMS/lubricant composite. Subsequently, the PDMS/lubricant composite was diluted with xylene in various ratios. The dilution ratio of the PDMS/lubricant composite to xylene was varied from 1 : 0 to 1 : 10 to produce mixtures of varying viscosities. The prepared mixture was magnetically

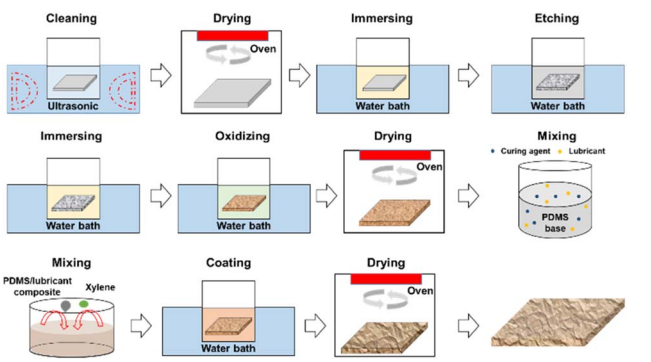

Fig. 1 Fabrication process of micro/nano-structured Al coated with PDMS/lubricant composite.

stirred at 300 rpm for one hour. After stirring, the Al specimens were immersed in the solution for five minutes. Finally, the coated Al specimens were placed on a tray and dried in an oven at 70 °C for more than three hours.

2.3 Experiments

The morphologies of the fabricated PDMS/lubricant composite coating surfaces were observed and analyzed by scanning electron microscopy (SEM, JSM-IT300, JEOL, Tokyo, Japan). The phase structures of the bare PDMS and PDMS/lubricant composite were analyzed using X-ray Diffraction (XRD, EMPyrean, PANalytical, Malvern, UK), whereas the quantitative and qualitative changes in the chemical composition of PDMS owing to the addition of the lubricant were analyzed using Fourier transform infrared spectroscopy (FTIR-ATR, Nicolet 6700, Thermo Scientific, Seoul, Republic of Korea). The surface roughness was measured more than thrice for each fabrication condition using a 2D profiler (SV-2100M4, Mitutoyo Co., Ltd, Kawasaki-shi, Japan), and the average roughness of the central line was calculated. The wettability of each specimen surface was determined by measuring the water droplet contact angle (WCA) and oil droplet contact angle (OCA). WCA and OCA were measured by placing 5 μL of water and oil at three random positions on the surface of the Al specimen coated with the PDMS composite, and the measurements were averaged. To measure the friction coefficients of the composite coatings with various surface structures, reciprocating sliding friction tests were conducted under dry and lubricated conditions (RFW 160, NEOPLUS Co., Ltd, Daejeon, Republic of Korea). For the dry condition, a steel ball with a diameter of 1 mm was selected as the counter tip, and the sliding stroke, sliding speed, vertical load, and number of sliding cycles were set to 2 mm, 4 mm s^{-1}, 50 mN, and 5000 cycles, respectively. For the lubricated condition, a steel ball with a diameter of 1 mm was chosen as the counter tip, and the sliding stroke, sliding speed, vertical load, and number of sliding cycles were set as 2 mm, 4 mm s^{-1}, 50 mN, and 10 000 cycles, respectively. The wear morphology was analyzed using SEM and a 2D profiler, and the wear rate was calculated by determining the wear width and depth. The wear rate is the volume of wear divided by the total sliding distance and vertical load. The tests were conducted more than three times under each condition to ensure the reliability of the friction coefficients, and wear rates were used.

3. Results and discussion

The aluminum surface was modified into micro/nanostructures and coated with a PDMS/lubricant composite, resulting in the fabrication of various surface morphologies, as illustrated in Fig. 2. Microstructures are formed during the etching process with hydrochloric acid, followed by the formation of nanostructures upon reaction with hot water, accompanied by hydrophilic modification. Scanning electron microscopy revealed that the etching process produced a three-dimensional hierarchical structure characterized by microscale roughness overlaid with nanoscale features. Microscale roughness

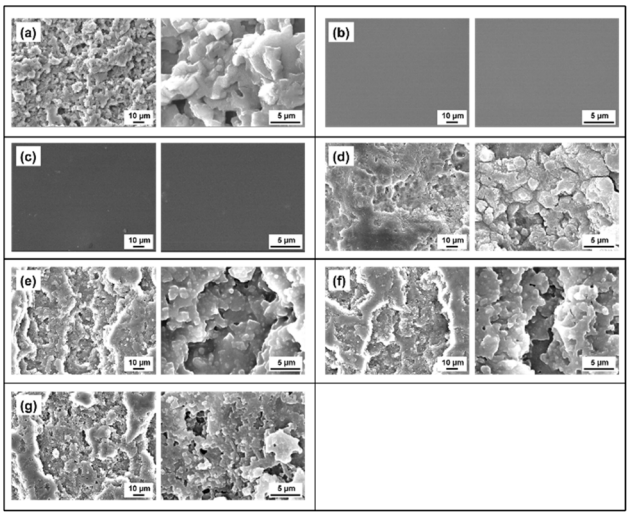

Fig. 2 SEM images of micro/nano-structured surfaces coated with PDMS/lubricant composites at varying xylene dilution ratios. Weight ratio of PDMS/lubricant composite: xylene is 1 to *X*, where *X* is (a) non-coating, (b) 0, (c) 1, (d) 3, (e) 5, (f) 7, (g) 10. (Left) Low magnification, (Right) high magnification.

predominantly formed at the boundaries of the polycrystalline aluminum surface, where etching occurred preferentially.[32] The boundaries, being more reactive than the particle interiors, facilitated faster etching rates and formation of microscale structures. Subsequent hot water treatment promoted the growth of nanosized boehmite γ-AlO (OH) platelets on a finely roughened surface.[33] Boehmite platelets formed perpendicularly on the surface when the aluminum oxide layers were hydrated in hot water. This hierarchical structure significantly increases the surface area and roughness of the aluminum substrate. The extent of the microstructure formation on the aluminum surface varied according to the mixing ratio of the PDMS/lubricant composite and xylene. Xylene, being a highly low-viscosity organic solvent, influenced the degree of structure formation based on its concentration. Consequently, microstructures with varying degrees of surface roughness are obtained. The surface morphologies can be classified into three types: surfaces fully coated with a smooth layer, surfaces coated only with microstructures, and surfaces coated only with nanostructures. At the lowest xylene mixing ratios (1 : 0 and 1 : 1), the PDMS/lubricant composite coating covered the entire surface and formed a smooth surface. At these ratios, the high viscosity of the PDMS/lubricant composite forms a coating layer that completely covers the micro/nanostructures, resulting in a smooth surface. As the mixing ratio exceeded 1 : 3, the microstructures gradually became evident, and at ratios above 1 : 7, all the microstructures were exposed. An increase in the xylene content reduced the viscosity, allowing the PDMS/lubricant composite to penetrate the micro/nanostructures more effectively, forming a hierarchical surface.

Fig. 3 displays the XRD patterns of bare PDMS and PDMS/lubricant composite. Both specimens exhibited characteristic peaks at $2\theta = 12°$, indicating the crystallinity of PDMS, which

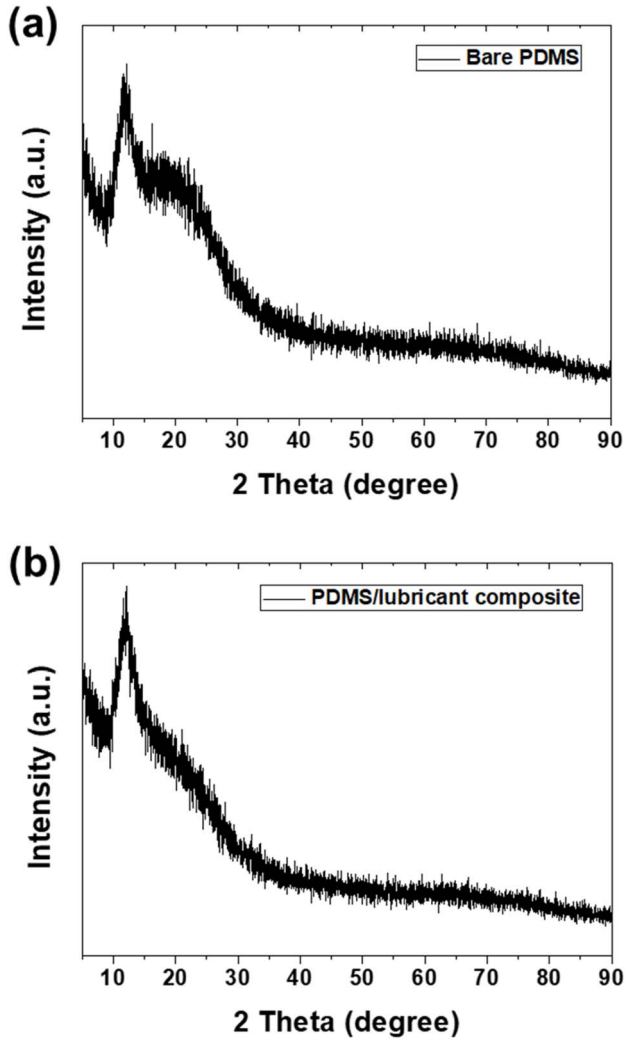

Fig. 3 Results of X-ray diffraction of (a) bare PDMS and (b) PDMS/lubricant composite.

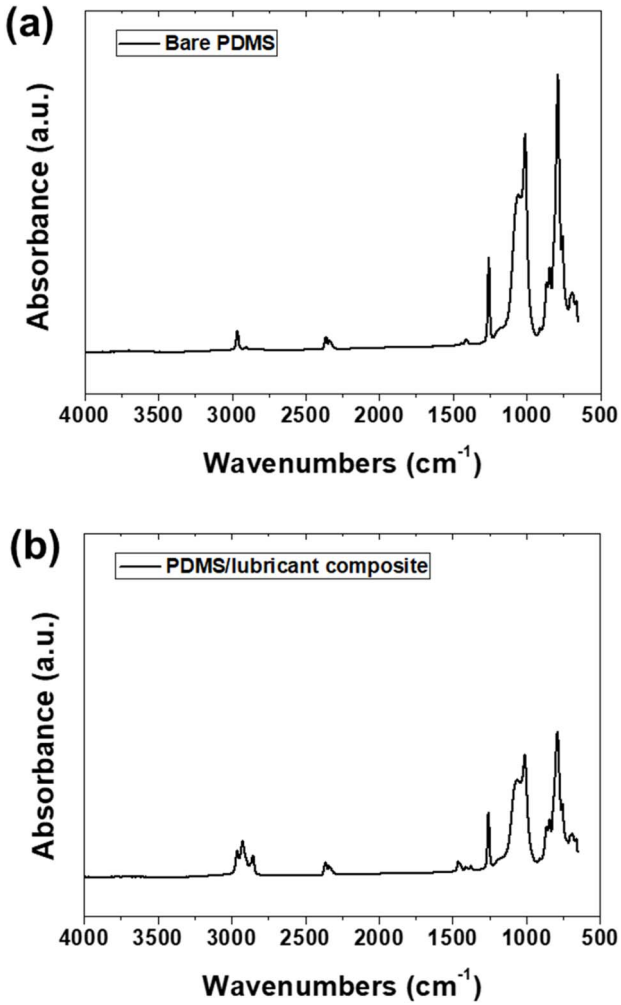

Fig. 4 Results of FTIR analysis of (a) bare PDMS and (b) PDMS/lubricant composite.

resulted from the regular arrangement of the PDMS molecules.[34] The similarity of the XRD pattern of the PDMS/lubricant composite to that of bare PDMS suggests that the addition of the lubricant does not significantly affect the crystal structure of PDMS. This indicates that the lubricant was uniformly dispersed within PDMS while maintaining its inherent properties.

Fig. 4 shows the FTIR spectra of bare PDMS and PDMS/lubricant composite. For bare PDMS, the peaks observed at 2962 and 2904 cm^{-1} are attributed to the asymmetric and symmetric stretching of CH_3, respectively, signifying the characteristic peaks of PDMS.[35] The strong peak at 1257 cm^{-1} represents the bending vibration of Si–CH_3, whereas the peaks at 1010 and 787 cm^{-1} correspond to the stretching vibrations of Si–O–Si.[36] The FTIR spectrum of the PDMS/lubricant composite shows peaks similar to those of bare PDMS, indicating that the chemical structure of PDMS is not significantly affected by the addition of the lubricant. However, the peaks at 2926 and 2855 cm^{-1} correspond to the asymmetric and symmetric stretching vibrations of CH_2 present in the lubricant, respectively, indicating successful mixing within the PDMS.[37] Additionally, the peak at 1066 cm^{-1} corresponds to the stretching vibration of Si–O–Si bonds, suggesting a slight decrease in the interactions between the PDMS molecular chains owing to the addition of the lubricant.[38] XRD and FTIR analyses confirmed that the PDMS/lubricant composite was a composite material in which the lubricant was successfully mixed, maintaining the inherent properties of PDMS while not significantly affecting its crystal and chemical structures. The addition of a lubricant indicates the stability and uniformity of the composite material without significantly affecting the crystal and chemical structures of PDMS.

Fig. 5 shows the surface characteristics of etched aluminum specimens coated with various ratios of xylene to the PDMS/lubricant composite. As observed in Fig. 5(a), an increase in the proportion of xylene correlated with an increase in surface roughness. The surface roughness of the non-coated specimen was measured at 3.13 μm, while the roughness values for the ratios of 1 : 0, 1 : 1, 1 : 3, 1 : 5, 1 : 7, and 1 : 10 were 0.63, 0.75, 1.76, 2.09, 2.79, and 3.04 μm, respectively. The highest

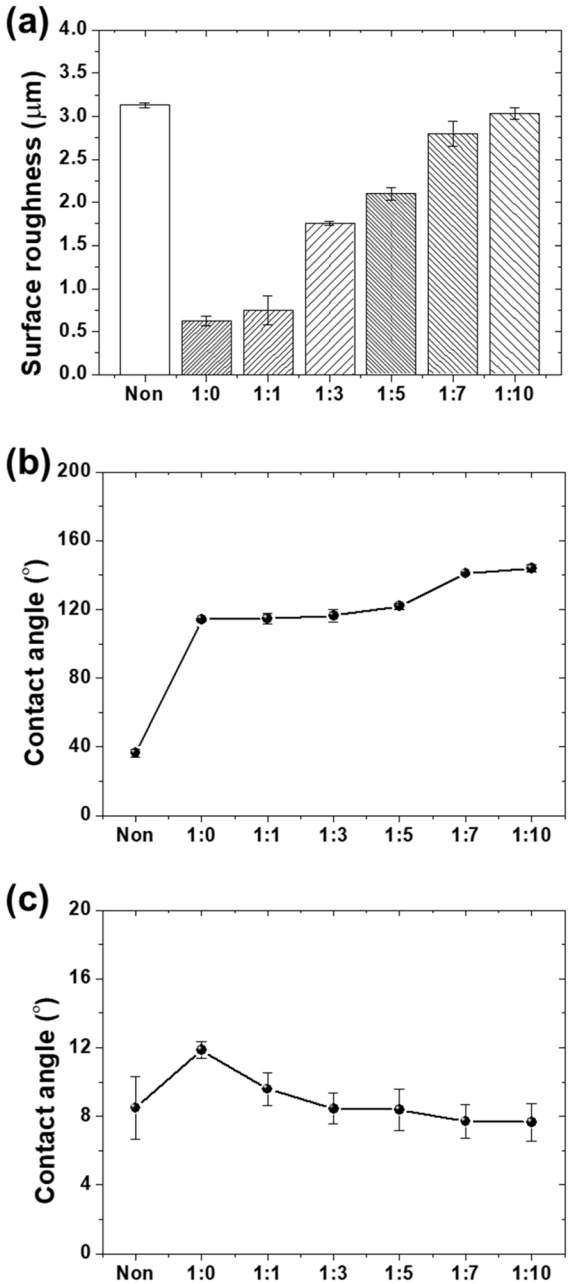

Fig. 5 Surface properties of micro/nano-structure surfaces coated with PDMS/lubricant composite at varying xylene dilution ratios: (a) surface roughness, (b) water contact angle and (c) oil contact angle.

roughness observed in the non-coated specimen can be attributed to the presence of a hierarchical structure.[39] In the cases of the 1 : 0 and 1 : 1 ratios, a significant reduction in surface roughness was observed, which can be ascribed to the high viscosity of the PDMS/lubricant composite filling the surface structures and forming a smooth coating layer. As the ratio of xylene increased, the surface roughness progressively approached the value of the non-coated specimen, indicating that the increased xylene content led to a reduction in the viscosity of the PDMS/lubricant composite, thereby exposing more micro/nanostructures. Fig. 5(b) presents the results of water contact angle (WCA) measurements. The WCA of the non-coated specimen was 36.4°, indicating a hydrophilic surface. The WCAs of the PDMS/lubricant composite-coated specimens significantly increased, ranging from 114.1° to 143.9°. The increase in WCA can be attributed not only to the hydrophobic characteristics of PDMS and the lubricant but also to the surface roughness introduced by the micro/nanostructures.[40] With an increase in the xylene ratio, it reached a maximum of 143.9° for the 1 : 10 specimen. This trend signifies the wetting behavior of rough hydrophobic surfaces, where increased surface roughness allows for the trapping of more air between the water droplet and the surface, thereby elevating the WCA.[41] Conversely, as shown in Fig. 5(c), the oil contact angle (OCA) exhibits an opposite trend to that of the WCA. The OCA of the non-coated specimen was 8.5°, indicating an oleophilic surface. The OCA values of the PDMS/lubricant composite-coated specimens varied depending on the xylene dilution ratio, ranging from 11.9° to 7.7°. The specimen with the highest xylene dilution ratio of 1 : 10 exhibited an OCA of 7.7°, which was lower than that of the non-coated specimen, indicating enhanced oleophilicity. An increase in surface roughness leads to an increase in the actual contact area between the oil droplet and the surface structure, enhancing diffusion and lowering the OCA. The changes in the wettability of the PDMS/lubricant composite-coated surfaces could be attributed to the dilution effect of xylene. As the xylene mixing ratio increased, the viscosity of the PDMS/lubricant composite decreased, facilitating easier penetration of the micro/nanostructures of the etched aluminum surface. At low xylene ratios, the high viscosity of the mixture limited the penetration into the surface structure, resulting in a smooth surface covering most of the micro/nanostructures. However, as the xylene ratio increased, the decreased viscosity allowed the mixture to adhere more effectively to the surface structure, thereby gradually exposing the micro-/nanostructures. The observed trends in the contact angles were attributed to the combined effects of surface chemistry and roughness.[42] PDMS is a material with low surface energy, exhibiting hydrophobicity, and its surface roughness increases with increasing xylene ratio. Consequently, the PDMS/lubricant composite coating effectively controlled the wettability of the etched aluminum surface. By adjusting the xylene ratio, it was possible to optimize the surface roughness and wettability, enabling the implementation of selective surfaces with coexisting hydrophobic and oleophilic properties.

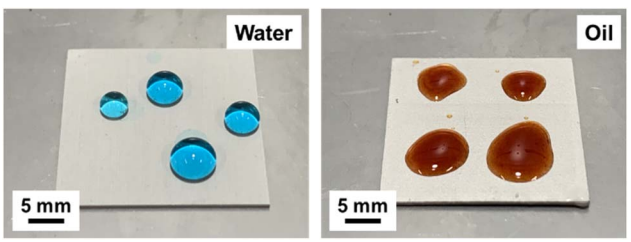

Fig. 6 Photographs of water and oil droplets on micro/nano-structured Al coated with PDMS/lubricant composite.

Fig. 6 shows the selective wettability of a specimen coated with the PDMS/lubricant composite on an etched aluminum surface. The water droplets retained their spherical shape on the coating, whereas the oil droplets spread to form a uniform film on the surface. This selective wettability is manifested by the combined effects of surface energy and microstructure. Hydrophobic surfaces tend to minimize the contact area with water droplets, whereas oleophilic surfaces aim to maximize the contact area with oil droplets. Consequently, the PDMS/lubricant composite coating exhibited unique surface characteristics that repelled water while also attracting oil. Selective wettability can be controlled by changing the xylene mixing ratio and the surface microstructure, thus offering valuable applications in various fields.

Fig. 7 shows the results of friction tests conducted under dry conditions. Fig. 7(a) illustrates the variation in the friction coefficient over 5000 cycles of the friction test. The non-coated specimen exhibited a high initial friction coefficient of 1.2, which decreased to 0.75 over 200 cycles, and then gradually increased to approximately 0.9 after 5000 cycles. The high initial friction coefficient can be attributed to the rough surface morphology of the etched Al, which leads to increased mechanical interlocking and deformation during the initial sliding cycles. The subsequent reduction in the friction coefficient was due to the formation of wear particles and the smoothing of the surface asperities. In contrast, the specimens coated with the PDMS/lubricant composite exhibited different friction coefficient trends. The ratios of 1 : 0 and 1 : 1 maintained low and stable friction coefficient of 0.08 and 0.15, respectively, throughout the friction test. This is a result of the formation of a stable lubrication film that effectively separates the sliding surfaces and reduces the adhesion and deformation. The slightly higher friction coefficient of the 1 : 1 specimen compared with that of the 1 : 0 specimen can be attributed to the increased surface roughness, leading to some degree of mechanical interlocking.[43] Specimens with ratios of 1 : 3, 1 : 5, 1 : 7, and 1 : 10 showed a sharp increase in the friction coefficient in the initial phase of the test, followed by a gradual increase to approximately 0.9 at 5000 cycles. The sharp increase in the friction coefficient is due to the thin coating thickness and increased exposure of the micro/nanostructures, leading to the easy removal of the PDMS/lubricant composite from the surface. As the sliding continued, the wear of the micro/nanostructures increased the surface roughness, leading to a gradual increase in the friction coefficient.[44] Fig. 7(b) shows the average friction coefficient measured for each specimen throughout the entire test period. The non-coated specimen had the highest average friction coefficient of 0.86, whereas the PDMS/lubricant composite-coated specimens exhibited lower values ranging from 0.08 to 0.71. The lowest average friction coefficient was observed for the 1 : 0 specimen, which indicated the formation of a stable and continuous lubricating film. The average friction coefficient increased with the xylene ratio, which was attributed to the decrease in the coating thickness and the increased exposure of the micro/nanostructures. Fig. 7(c) shows the wear rate of each specimen, calculated from the wear volume, normal load, and total sliding distance.

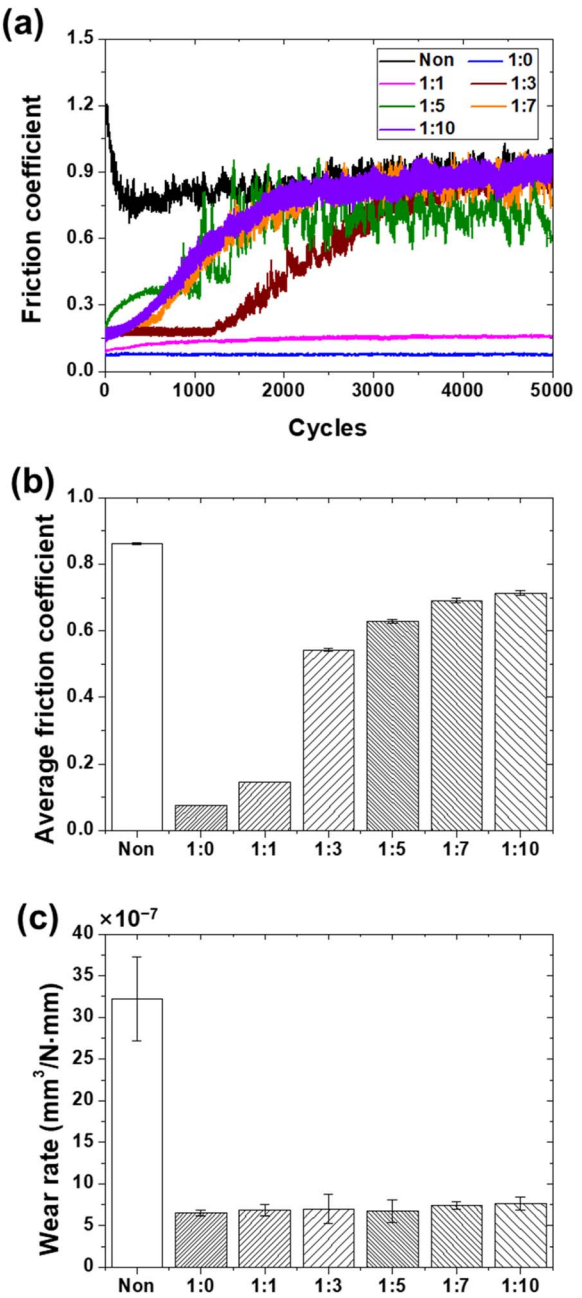

Fig. 7 Friction and wear characteristics of micro/nano-structure surfaces coated with PDMS/lubricant composite at varying xylene dilution ratios under dry condition: (a) friction coefficient history, (b) average friction coefficient and (c) wear rate.

The non-coated specimen exhibited the highest wear rate of 3.23×10^{-6} mm^3 N^{-1} mm^{-1}, which is indicative of severe wear due to direct contact between the rough aluminum surface and the counter tip. Specimens coated with PDMS/lubricant composite demonstrated lower wear rates ranging from 6.46×10^{-7} mm^3 N^{-1} mm^{-1} to 7.62×10^{-7} mm^3 N^{-1} mm^{-1}. The lowest wear rate was observed in the 1 : 0 specimen, which was attributed to the formation of a stable and continuous lubrication film that effectively protected the surface from wear. The wear rate increased slightly with the xylene ratio owing to

a decrease in the coating thickness and an increase in the exposure of micro/nanostructures, thereby increasing the contact area with the counter tip. Consequently, the superior friction and wear performances of the PDMS/lubricant composite coatings under dry conditions can be attributed to various factors. The presence of a lubricant in the composite coating provides a low-shear interface between the sliding surfaces, reducing adhesive friction.[45] Lubricant molecules can easily shear against each other, minimizing resistance against sliding motion. The micro/nanostructures on the coated surface could store the lubricant, replenish the sliding interface, and maintain a stable lubrication film. This prevents direct contact between the mating surfaces, further reducing the friction and wear. Additionally, PDMS is known for its low elastic modulus and high elasticity, which allows it to deform elastically under a load.[46] This elastic deformation helps distribute the contact stress more evenly across the surface, thereby reducing the localized stress concentration. The differences in friction and wear performance across various xylene ratios were attributed to differences in the coating thickness and surface morphology. At lower xylene ratios, the coating was thicker and more uniform, forming a stable lubrication film that effectively protected the Al substrate. However, as the xylene ratio increased, the coating became thinner and less uniform, exposing more micro-/nanostructures. These exposed structures can still store lubricants, but the increased surface roughness leads to higher contact stress and enhanced abrasive wear.

The wear morphology of the surface was observed following the friction tests conducted under dry conditions, as illustrated in Fig. 8. In the case of the non-coated specimen, wide and deep wear tracks were observed. Deep grooves and cracks were present within these wear tracks, and deformed aluminum was observed to have been pushed up to the edges of the wear tracks. This indicated that the hard wear particles penetrated the soft aluminum matrix, resulting in abrasive wear mechanisms such as cutting, plowing, and wedge formation.[47] The presence of deep grooves and cracks suggests that the wear mechanism is dominated by plastic deformation and fracture. The deformed aluminum pushed to the edges of the tracks is a typical characteristic of plowing, where the hard asperities of the counter tip penetrate the softer aluminum surface and move the material laterally. Additionally, the presence of wear particles indicates that repetitive plastic deformation leads to the formation and propagation of subsurface cracks, resulting in delamination wear where thin sheets of material are separated. In contrast, specimens coated with a PDMS/lubricant composite showed narrower and shallower wear tracks compared to non-coated aluminum. The specimen with the lowest xylene dilution ratio and thickest coating (1 : 0) showed no noticeable wear on the aluminum substrate, with only delamination and scratches on the coating layer. This indicates that the PDMS/lubricant composite coating effectively protected the aluminum surface from direct contact with the counter tip, thereby reducing wear. The presence of scratches suggests mild wear resulting from the hard surface of the counter tip scratching the softer PDMS/lubricant composite coating. As the xylene dilution ratio increased, the wear tracks became wider and deeper, indicating the increased wear of the coating and exposure of the aluminum substrate. However, the wear tracks were narrower and shallower than those of non-coated aluminum, suggesting that the PDMS/lubricant composite coating provided significant protection against wear. In the specimens with dilution ratios of 1 : 7 and 1 : 10, the aluminum substrate was partially exposed and abrasive wear with scratches was observed. The presence of scratches suggests that the primary wear mechanism is abrasion, with the hard asperities of the counter-tip surface abrading the softer aluminum surface. However, the absence of deep grooves and cracks indicated that the PDMS/lubricant composite coating provided some level of protection, thereby reducing the acceleration of wear. Thus, the PDMS/lubricant composite coating demonstrated excellent wear resistance under dry conditions regardless of the xylene dilution ratio. As the xylene ratio increased, the coating thickness decreased, exposing the aluminum substrate to wear. However, this coating could prevent wear acceleration. The specimen with the lowest xylene ratio and thickest coating (1 : 0) showed only light wear on the coating and no noticeable wear on the aluminum substrate, exhibiting the best wear resistance.

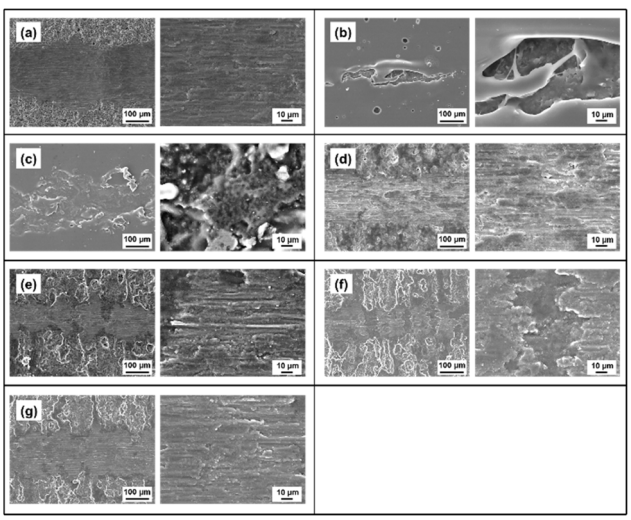

Fig. 8 SEM images of wear tracks on micro/nano-structured surfaces coated with PDMS/lubricant composite at varying xylene dilution ratios under dry conditions. Weight ratio of PDMS/lubricant composite: xylene is 1 to *X*, where *X* is (a) non-coating, (b) 0, (c) 1, (d) 3, (e) 5, (f) 7, (g) 10. (Left) Low magnification, (Right) high magnification.

Fig. 9 illustrates the variation in the friction coefficient during the friction test conducted under lubricated conditions for 10 000 cycles. The friction coefficients for the specimens without coating and with ratios of 1 : 3, 1 : 5, 1 : 7, and 1 : 10 began at a low value of approximately 0.2, but experienced a rapid increase before reaching 1000 cycles. Subsequently, it gradually decreased to reach about 0.3. The initial low friction coefficient can be attributed to the lubricating effect of the oil, which forms a protective layer between sliding surfaces. However, as the sliding continued, the lubrication layer was disrupted, leading to contact between the aluminum substrate

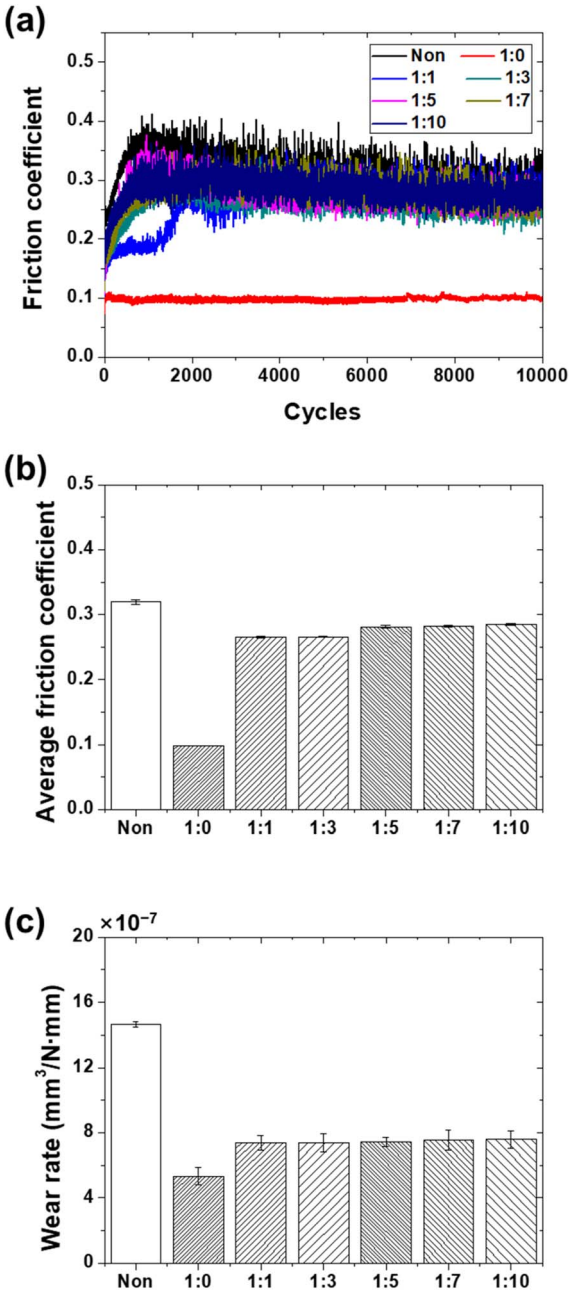

Fig. 9 Friction and wear characteristics of micro-nanostructure surfaces coated with PDMS/lubricant composite at varying xylene dilution ratios under lubrication condition: (a) friction coefficient history, (b) average friction coefficient and (c) wear rate.

and the counter tip, which resulted in a sharp increase in the friction coefficient. The subsequent gradual decrease in the friction coefficient can be attributed to the run-in process, where the surface asperities become smoother and a stable lubrication layer is formed.[48] In the case of the 1 : 1 specimen, the friction coefficient started at 0.2 and after 1000 cycles, it rapidly increases to approximately 0.3, and then maintains a relatively stable value. The initial low friction coefficient was due to the combined lubricating effect of the oil and PDMS/lubricant composite. The sharp increase in the friction coefficient after 1000 cycles can be attributed to the partial wear of the PDMS/lubricant composite and exposure of the micro/nanostructures. The relatively stable friction coefficient after the initial increase can be attributed to the balance between the lubricating effect of the oil and the exposed micro/nanostructures. The 1 : 0 specimen exhibited a stable and low friction coefficient of approximately 0.1 throughout the test. This can be attributed to the formation of a stable lubrication layer by the PDMS/lubricant composite, which was further enhanced in the presence of the oil. The thick and uniform coating of the 1 : 0 specimen provided effective protection against wear and maintained a low friction coefficient. As seen in Fig. 9(b), the average friction coefficient for the 1 : 0 specimen was the lowest at 0.09, while the non-coated and other PDMS/lubricant composite-coated specimens showed relatively higher values of 0.27–0.32. The low average friction coefficient of the 1 : 0 specimen can be attributed to the synergistic effect of the PDMS/lubricant composite and the oil in forming a stable lubrication layer. The higher average friction coefficients for the non-coated and other coated specimens can be attributed to the increased contact between the substrate and counter tip, resulting from the disruption of the lubrication layer and exposure of the micro/nanostructures. Fig. 9(c) illustrates the wear rate of each specimen under lubricated conditions. The highest wear rate was observed in the non-coated specimen, at 1.47×10^{-6} mm^3 N^{-1} mm^{-1}, whereas the PDMS/lubricant-coated specimens exhibited a lower wear rate, ranging from 5.32×10^{-7} to 7.58×10^{-7} mm^3 N^{-1} mm^{-1}. The elevated wear rate of the non-coated specimen could be attributed to the direct contact between the rough aluminum surface and counter tip, leading to severe abrasive and adhesive wear. The reduced wear rate in the PDMS/lubricant composite coating specimens may be ascribed to the formation of a protective lubrication film, which minimized wear by reducing the direct contact between the aluminum substrate and counter tip. The specimen with a ratio of 1 : 0 demonstrated the lowest wear rate, at 5.32×10^{-7} mm^3 N^{-1} mm^{-1}, likely due to the thick and uniform application of the PDMS/lubricant composite, providing effective protection against wear. Under lubricated conditions, the PDMS/lubricant composite coating showed improved friction and wear performance compared with the non-coated coating. This enhancement may be due to the synergistic effect of the coating and lubricant. The micro/nanostructures on the coating surface serve to store both the lubricant within the coating and the additional lubricant, continuously supplying the lubricant to the contact interface during sliding, thus establishing a stable lubrication film.[49] The presence of this lubrication film prevents direct contact between the mating surfaces, reducing adhesive friction and wear. Additionally, the oleophilic properties of PDMS promote the formation of a lubrication film. The low surface energy of PDMS enables the oil to spread easily and form a uniform lubrication film, which helps to evenly distribute the contact stress and minimize surface wear.[50] Furthermore, the elastic deformation of PDMS under an applied load accommodates surface irregularities and aids in maintaining a stable lubricating film. The variation in friction and wear behaviors with

different xylene ratios is attributed to differences in the coating thickness and surface morphology, similar to dry conditions. At lower xylene ratios, a thicker and more uniform coating provided a stable lubrication film and an effective protective function, leading to reduced friction coefficients and wear rates. However, as the xylene ratio increased, the coating became thinner and less uniform, exposing more micro/nanostructures. While these structures can retain the lubricant, the increased surface roughness leads to higher contact stress and abrasive wear, progressively increasing the friction coefficient and wear rate. It is noteworthy that even at higher xylene ratios, under lubricated conditions, the PDMS/lubricant composite coating demonstrated superior performance in reducing friction and wear compared to the non-coated aluminum surface. This underscores the effectiveness of the composite coating in enhancing the friction and wear characteristics of the aluminum surface, even with thinner coatings and exposed micro-/nanostructures.

The wear morphology of the surfaces was observed following the friction tests under lubricated conditions, as depicted in Fig. 10. For the non-coated specimen, extensive and deep wear tracks were discernible, indicating severe wear. Within these wear tracks, the presence of deep grooves and cracks suggests mechanisms of abrasive wear and surface fatigue. In contrast, specimens coated with the PDMS/lubricant composite exhibited significantly reduced wear compared to the non-coated specimen, with narrower and shallower wear tracks, thereby demonstrating that the PDMS/lubricant composite coating effectively protects the aluminum surface from wear. As the dilution ratio of xylene increased, the wear tracks became slightly wider and deeper, suggesting an increase in the wear of the coating and the exposure of the aluminum substrate. However, even at the highest xylene ratio, the wear tracks remained narrower and shallower than those of the non-coated specimens, indicating that the PDMS/lubricant composite coating provided substantial protection against wear. Thus, the PDMS/lubricant composite coating significantly enhanced the wear resistance of aluminum surfaces under lubricated conditions. The coating acts as a protective barrier between the sliding surfaces, reducing the direct contact between the aluminum substrate and counter tip, thereby preventing accelerated wear. With an increase in the xylene ratio, a reduction in the coating thickness led to an increased exposure of the micro/nanostructures and increased wear. Nevertheless, even at the highest xylene ratio, the PDMS/lubricant composite coating continued to offer superior wear resistance compared with the non-coated specimen. The specimen with the thickest coating at a 1 : 0 ratio demonstrated excellent wear resistance, preventing severe wear of the aluminum substrate.

Fig. 11 presents a schematic illustration of the wear mechanisms observed on the non-coated and PDMS/lubricant composite-coated aluminum surfaces under dry and lubricated conditions. For the non-coated specimen (Fig. 11(a)), under dry conditions, the contact between the rough aluminum surface and counter tip results in severe abrasive and adhesive wear. The hard asperities of the counter tip penetrated the softer aluminum surface, leading to plowing, cutting, and delamination wear. Plowing occurs when hard asperities plastically deform the aluminum surface, pushing the material aside and forming ridges. Cutting involves the removal of material in the form of chips owing to the penetration of sharp asperities. Delamination wear occurs when repeated plastic deformation leads to subsurface crack initiation and propagation, causing removal of sheet-like wear debris. Under lubricated conditions, the presence of a lubricant reduces direct contact; however, disruption of the lubricant film can lead to abrasive wear and surface fatigue. Abrasive wear occurs when the hard asperities of the counter tip abrade the aluminum

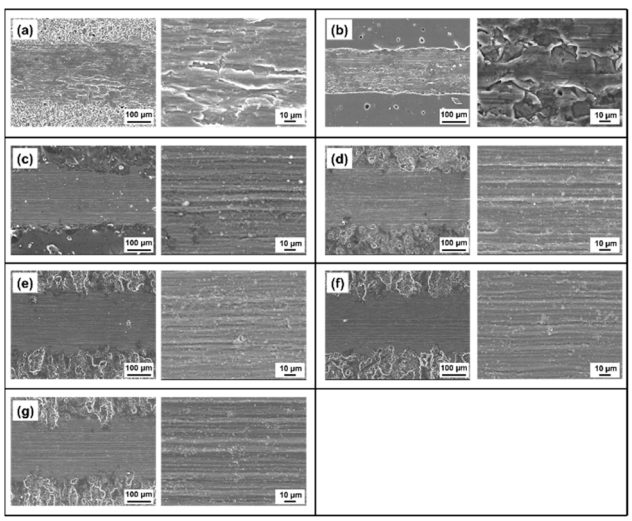

Fig. 10 SEM images of wear tracks on micro/nano-structured surfaces coated with PDMS/lubricant composite at varying xylene dilution ratios under lubrication conditions. Weight ratio of PDMS/lubricant composite: xylene is 1 to *X*, where *X* is (a) non-coating, (b) 0, (c) 1, (d) 3, (e) 5, (f) 7, (g) 10. (Left) Low magnification, (Right) high magnification.

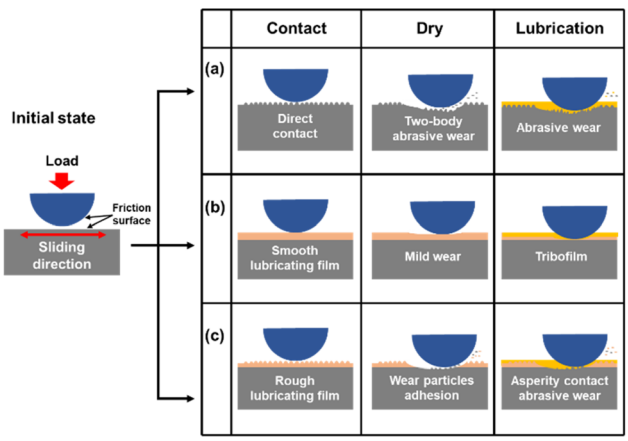

Fig. 11 Schematic illustration of the wear mechanisms on (a) non-coating, (b) lower xylene ratio (1 : 0 and 1 : 1), and (c) higher xylene ratio (1 : 3, 1 : 5, 1 : 7, and 1 : 10) PDMS/lubricant composite-coated aluminum surfaces under dry and lubricated conditions.

surface, whereas surface fatigue results from repeated stress cycles, which causes crack initiation and propagation.

For the specimens with lower xylene ratios (1 : 0 and 1 : 1) (Fig. 11(b)), under dry conditions, the thick and uniform PDMS/lubricant composite coating acted as a sacrificial layer, preventing direct contact between the aluminum substrate and counter tip. The coating underwent mild abrasive wear and delamination, which protected the underlying aluminum from severe wear. Abrasive wear of the coating occurs when the hard asperities of the counter tip abrade the softer coating material, whereas delamination wear involves the removal of coating fragments owing to the subsurface crack propagation. Under lubricated conditions, the synergistic effect of the coating and lubricant forms a stable lubrication film, minimizing wear by reducing direct contact and distributing the contact stress. The lubricant film prevents the penetration of hard asperities and reduces the adhesion between the mating surfaces, whereas the elastic deformation of the PDMS matrix helps to accommodate surface irregularities and maintain the lubricant film.

In the case of the specimens with higher xylene ratios (1 : 3, 1 : 5, 1 : 7, and 1 : 10) (Fig. 11(c)), under dry conditions, the thinner and less uniform coating led to partial exposure of the micro/nanostructures. The exposed structures experienced abrasive wear owing to the penetration and plowing action of the hard asperities; however, the coating still provided some protection, preventing severe wear acceleration. The coating remnants and micro-/nanostructures work together to trap wear debris and reduce the severity of abrasive wear. Under lubricated conditions, the exposed structures can store lubricants, thereby contributing to the formation of a lubricating film. However, the increased surface roughness resulted in a higher contact stress and abrasive wear compared to the 1 : 0 specimen. The lubricant film is more easily disrupted owing to the surface roughness, leading to more frequent asperity contact and abrasion. Nevertheless, the combined action of the coating and lubricant still reduced wear compared with the non-coated specimen by providing a protective layer and maintaining a partial lubrication film.

In conclusion, the PDMS/lubricant composite coating significantly altered the wear mechanisms of aluminum surfaces by serving as a protective layer, reducing direct contact, and working synergistically with lubricants to form stable lubricating films. The coating thickness and uniformity, which are controlled by the xylene ratio, determine the extent of protection and interaction between the coating, lubricant, and surface structures. Understanding these wear mechanisms provides valuable insights into the tribological behavior of composite coatings and aids in the development of optimized coating systems for enhanced wear resistance.

Fig. 12 illustrates the self-cleaning effects of the PDMS/lubricant composite coating on aluminum surfaces etched with micro/nanostructures. The images display the surface before and after the application of the water droplets at a tilt angle of 20°. Initially, the surface was contaminated by a substantial amount of dust particles. However, as water droplets roll off the surface, dust particles are collected and removed, thereby effectively cleaning the surface. This self-cleaning effect is attributed to the combination of the hierarchical micro/nanostructures and hydrophobic PDMS/lubricant composite coatings. Micro/nanostructures trap air pockets between the water droplets and the surface, enhancing surface hydrophobicity and inducing a Cassie–Baxter state.[51] In which water droplets rest atop the micro/nanostructures, allowing them to easily roll off the surface and remove contaminants. The PDMS/lubricant composite coating further enhanced the hydrophobicity owing to its low surface energy, and the lubricant reduced the adhesion of contaminants.

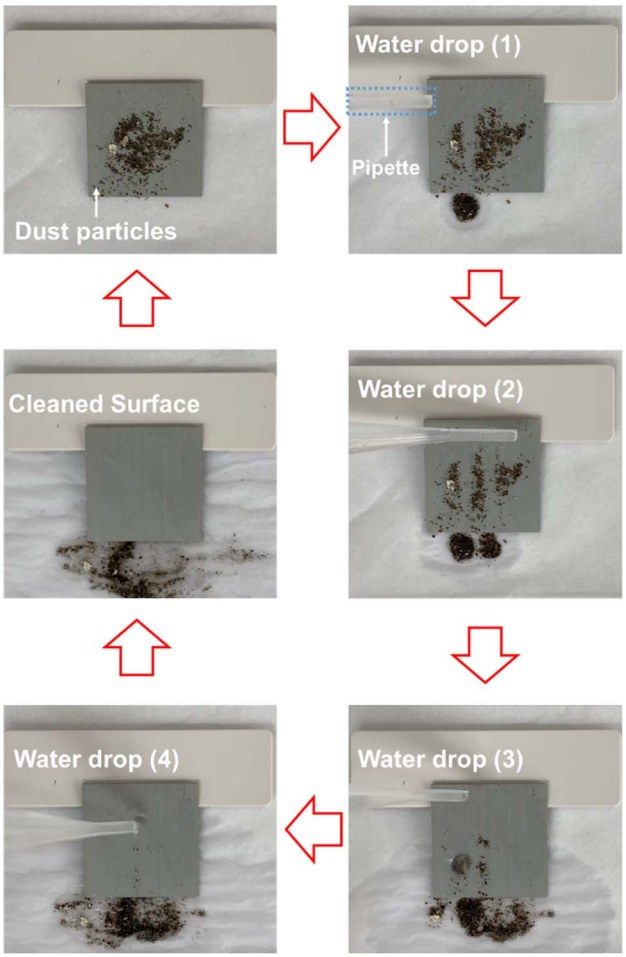

Fig. 12 Self-cleaning test of micro/nano-structured Al coated with PDMS/lubricant composite.

Fig. 13 shows the behavior of the water and oil droplets on the PDMS/lubricant composite-coated surface at a tilt angle of 20°. The blue-dyed water droplets easily rolled off the surface, demonstrating the hydrophobicity of the coating. In contrast, the red-dyed oil droplets remained adhered to the surface, indicating the oleophilic characteristics of the coating. The different behaviors of water and oil droplets on the coating surface stem from the differences in the surface tension and the interactions between the liquids and the coating.[52] Water has a high surface tension and forms a large contact angle on the PDMS/lubricant composite-coated surface. On the other hand, oil has low surface tension and forms a low contact angle,

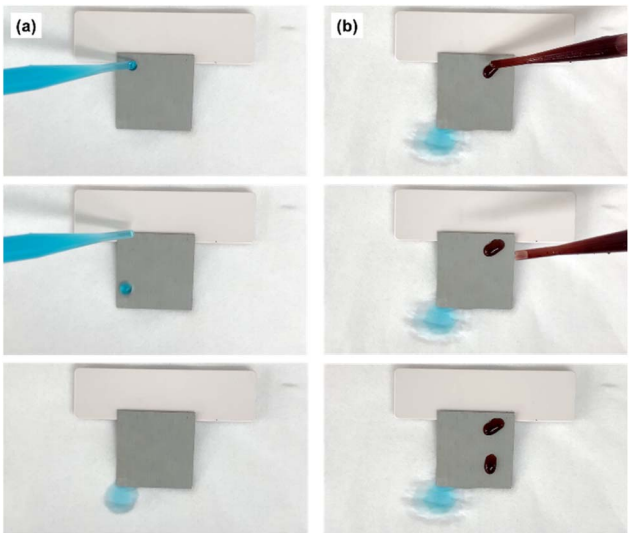

Fig. 13 Comparison of the wettability of water and oil droplets on micro/nano-structured Al coated with PDMS/lubricant composite: (a) water droplet, (b) oil droplet.

causing the oil droplets to spread and increase adhesion to the coating.

The results and analyses presented in this study demonstrate the effectiveness of the PDMS/lubricant composite coating in enhancing the frictional and wetting properties of aluminum. This coating significantly reduces friction and wear under both dry and lubricated conditions owing to the formation of a stable lubricating film and the wear resistance provided by the PDMS matrix. The hierarchical micro/nanostructures created by the etching process further enhanced hydrophobicity and self-cleaning capability. The selective wettability of the coating towards water and oil offers various advantages, including contamination prevention on surfaces, wear prevention due to lubricant oxidation and performance degradation, and improved corrosion resistance.[53–55] The findings of this study are expected to contribute to the development of lightweight technologies and enhance the durability/wear resistance of mechanical components, potentially affecting the mechanical industry.

4. Conclusions

In this study, a hierarchical PDMS/lubricant composite coating was successfully developed and applied to etched aluminum surfaces to enhance their friction/wear performance and selective wettability. The coating was prepared by mixing PDMS, lubricant, and xylene in various ratios, and depositing them on aluminum substrates with micro/nanostructures formed by chemical etching. The etching process created a hierarchical surface structure on the aluminum substrate, and the coating with the PDMS/lubricant composite resulted in various surface morphologies depending on the xylene dilution ratio. XRD and FTIR analyses confirmed the successful incorporation of the lubricant into the PDMS matrix without significantly altering its chemical composition. The PDMS/lubricant composite coating exhibited excellent hydrophobicity and oleophilicity, with the surface wettability varying according to surface chemistry and roughness. The coating significantly reduced the friction coefficient and wear rate compared to the etched aluminum surface, with the specimen having the lowest xylene ratio demonstrating the best friction and wear performance. The self-cleaning ability of the coating was demonstrated by the efficient removal of contaminants using water droplets, and selective wettability was demonstrated through the repellence of water and the spreading of oil on the surface. Wear morphology analysis revealed that the coating effectively protected the aluminum substrate from wear under both the dry and lubricated conditions. In conclusion, the hierarchical PDMS/lubricant composite coating provides a solution for improving the friction performance, self-cleaning ability, and selective wettability of aluminum surfaces. The multifunctional characteristics of this coating open new possibilities for various industrial applications, and future research should focus on optimizing the coating structure.

Data availability

The datasets generated and analyzed during the current study are available within the manuscript itself. All relevant data are presented in the form of figures, tables, and supplementary information accompanying this article.

Author contributions

Sung-Jun Lee: conceptualization, methodology, software, validation, formal analysis, investigation, data curation, writing – original draft, writing – review & editing, visualization. Dawit Zenebe Segu: commented on manuscript, resources, validation. Chang-Lae Kim: conceptualization, methodology, resources, writing – review & editing, supervision, project administration.

Conflicts of interest

There are no conflicts to declare.

Acknowledgements

This results was supported by “Regional Innovation Strategy (RIS)” through the National Research Foundation of Korea (NRF) funded by the Ministry of Education (MOE) (2021RIS-002). This work was supported by the National Research Foundation of Korea (NRF) grant funded by the Korea government (MSIT) (No. RS-2023-00219369, RS-2024-00349019).

References

1 M. Soori, B. Arezoo and R. Dastres, *Cognit. Rob.*, 2023, **3**, 54–70.
2 W. Wu, R. Xia, G. Qian, Z. Liu, N. Razavi, F. Berto and H. Gao, *Prog. Mater. Sci.*, 2023, **131**, 101021.

3 V. Ogbonna, A. Popoola and O. Popoola, *Polym. Bull.*, 2023, **80**, 3449–3487.
4 M. Álvarez, D. Ferrández, P. Guijarro-Miragaya and C. Morón, *Materials*, 2023, **16**, 872.
5 U. De Maio, F. Greco, R. Luciano, G. Sgambitterra and A. Pranno, *Mech. Res. Commun.*, 2023, **128**, 104045.
6 G. Kaplan and M. A. Salem Elmekahal, *Environ. Sci. Pollut. Res.*, 2021, **28**, 52936–52962.
7 W. Zhang and J. Xu, *Mater. Des.*, 2022, **221**, 110994.
8 C. Delprete and A. Razavykia, *Int. J. Engine Res.*, 2020, **21**, 725–741.
9 J. Domitner, Z. Silvayeh, A. S. Sabet, K. I. Öksüz, L. Pelcastre and J. Hardell, *J. Manuf. Process.*, 2021, **64**, 774–784.
10 P. Podrabinnik, I. Gershman, A. Mironov, E. Kuznetsova and P. Peretyagin, *Lubricants*, 2020, **8**, 24.
11 M. Azadi and M. S. A. Parast, *Data Brief*, 2022, **41**, 107984.
12 P. Zhang, L. Zeng, X. Mi, Y. Lu, S. Luo and W. Zhai, *Wear*, 2021, **474**, 203760.
13 H. Guo, J. Pang, A. R. Adukure and P. Iglesias, *Tribol. Lett.*, 2020, **68**, 1–10.
14 Y. Zhang, Y. Zhang, S. Zhang, G. Yang, C. Gao, C. Zhou, C. Zhang and P. Zhang, *Tribol. Int.*, 2020, **141**, 105890.
15 C. Kumara, L. Speed, M. B. Viola, H. Luo and J. Qu, *ACS Sustain. Chem. Eng.*, 2021, **9**, 7198–7205.
16 Y. Zhang, Z. Ma, Y. Feng, Z. Diao and Z. Liu, *Energies*, 2021, **14**, 2320.
17 A. Thornley, Y. Wang, C. Wang, J. Chen, H. Huang, H. Liu, A. Neville and A. Morina, *Tribol. Int.*, 2022, **168**, 107437.
18 G. Vaitkunaite, C. Espejo, C. Wang, B. Thiebaut, C. Charrin, A. Neville and A. Morina, *Tribol. Int.*, 2020, **151**, 106531.
19 G. Vaitkunaite, C. Espejo, B. Thiebaut, A. Neville and A. Morina, *Tribol. Int.*, 2022, **171**, 107551.
20 L. Meijun, L. Xu, C. Zhu, Z. Li and S. Wei, *J. Mater. Res. Technol.*, 2023, **28**, 752–773.
21 H. Wang, L. Tian, J. Zheng, D. Yang and Z. Zhang, *Tribol. Int.*, 2022, **173**, 107657.
22 L. B. Boinovich, A. M. Emelyanenko, A. D. Modestov, A. G. Domantovsky and K. A. Emelyanenko, *ACS Appl. Mater. Interfaces*, 2015, **7**, 19500–19508.
23 J. Zhu, Y. Shan, T. Wang, H. Sun, Z. Zhao, L. Mei, Z. Fan, Z. Xu, I. Shakir and Y. Huang, *Nat. Commun.*, 2016, **7**, 13432.
24 Y. Ouyang, X. Xia, H. Ye, L. Wang, X. Jiao, W. Lei and Q. Hao, *ACS Appl. Mater. Interfaces*, 2018, **10**, 3549–3561.
25 S. Ghosh, S. K. Sharma, S. Rana, T. S. Khan, T. Sasaki, S. S. Acharyya and R. Bal, *ACS Appl. Nano Mater.*, 2023, **6**, 17668–17680.
26 X. Li, Z. Chen, A. Li, Y. Yu, X. Chen and H. Song, *ACS Appl. Mater. Interfaces*, 2020, **12**, 48718–48728.
27 J. Li, N. Zhang and D. H. Ng, *J. Mater. Chem. A*, 2015, **3**, 21106–21115.
28 W. Wang, W. Zhao, K. Wang, L. Wang, X. Wang, S. Wang, C. Zhang and J. Bai, *Appl. Surf. Sci.*, 2017, **416**, 710–715.
29 Y. Lu, *Tribol. Int.*, 2018, **119**, 131–142.
30 K. Ziegler-Skylakakis, J. Fabri, U. Graeser and T. Simo, *Xylenes*, Acerican Cancer Society, 2019, pp. 1–20.
31 W. J. Cannella, *Kirk-Othmer Encyclopedia of Chemical Technology*, 2000.
32 T. Shi, J. Liang, X. Li, C. Zhang and H. Yang, *Polymers*, 2022, **14**, 4509.
33 C. Wang, Y. Lyu, J. Li, L. Li, T. Li, J. Yang, N. Xing and X. Zhang, *ACS Appl. Nano Mater.*, 2022, **5**, 3201–3212.
34 S.-J. Lee, G.-M. Kim and C.-L. Kim, *Polym. Test.*, 2023, **117**, 107855.
35 S.-J. Lee, G.-M. Kim and C.-L. Kim, *RSC Adv.*, 2023, **13**, 3541–3551.
36 J. C. Almeida, A. G. Castro, I. M. M. Salvado, F. M. Margaça and M. H. V. Fernandes, *Mater. Lett.*, 2014, **128**, 105–109.
37 G. Mazzon, M. Zahid, J. A. Heredia-Guerrero, E. Balliana, E. Zendri, A. Athanassiou and I. S. Bayer, *Appl. Surf. Sci.*, 2019, **490**, 331–342.
38 Y. Liu, Q. Lin, J. Chen, Y. Shao, Y. Wang and J. Wang, *Colloids Surf., A*, 2022, **648**, 129279.
39 W. Li, H. Yang, S. Xue, T. Shi, Q. Wang and H. Peng, *Appl. Phys. A: Mater. Sci. Process.*, 2022, **128**, 626.
40 S. Kim, H. J. Hwang, H. Cho, D. Choi and W. Hwang, *Chem. Eng. J.*, 2018, **350**, 225–232.
41 T. L. Liu, Z. Chen and C.-J. Kim, *Soft Matter*, 2015, **11**, 1589–1596.
42 J. Wang, Y. Wu, Y. Cao, G. Li and Y. Liao, *Colloid Polym. Sci.*, 2020, **298**, 1107–1112.
43 S.-J. Lee and C.-L. Kim, *Soft Matter*, 2024, **20**, 1467–1474.
44 M. Afshar-Mohajer, X. Yang, R. Long and M. Zou, *Tribol. Int.*, 2022, **165**, 107271.
45 Z. Zhao, X. Fan, W. Li, Y. He, Q. Sun and M. Zhu, *Appl. Surf. Sci.*, 2022, **604**, 154571.
46 S.-J. Lee and C.-L. Kim, *RSC Adv.*, 2023, **13**, 33595–33602.
47 A. Rosenkranz, H. L. Costa, M. Z. Baykara and A. Martini, *Tribol. Int.*, 2021, **155**, 106792.
48 R. Zhang, Q. Chen, X. Fan, Z. He, L. Xiong and M. Shen, *Langmuir*, 2020, **36**, 3887–3893.
49 W. Huang, L. Jiang, C. Zhou and X. Wang, *Tribol. Int.*, 2012, **52**, 87–93.
50 D. Wu, S.-z. Wu, Q.-D. Chen, S. Zhao, H. Zhang, J. Jiao, J. A. Piersol, J.-N. Wang, H.-B. Sun and L. Jiang, *Lab Chip*, 2011, **11**, 3873–3879.
51 C. E. Cansoy, H. Y. Erbil, O. Akar and T. Akin, *Colloids Surf., A*, 2011, **386**, 116–124.
52 B. Li, J. Bai, J. He, C. Ding, X. Dai, W. Ci, T. Zhu, R. Liao and Y. Yuan, *Coatings*, 2023, **13**, 301.
53 H. Li and X. Guo, *J. Cleaner Prod.*, 2024, **439**, 140857.
54 M. Hegde, J. Mohan, M. Q. M. Warraich, Y. Kavanagh, B. Duffy and E. F. Tobin, *Wear*, 2023, **524**, 204766.
55 X. Huang, Q. Weng, Y. Chen, L. Zhang and X. Sheng, *Surf. Interfaces*, 2024, **45**, 103911.